

THE KOMAN DAWSONITE AND REALGAR–ORPIMENT DEPOSIT, NORTHERN ALBANIA: INFERENCES ON PROCESSES OF FORMATION

VINCENZO FERRINI[§]

Dipartimento di Scienze della Terra, Università degli Studi di Roma “La Sapienza”, P.le A. Moro, 5, I-00185 Roma, Italy

LUCIO MARTARELLI

Centro di Studio per gli Equilibri Sperimentali in Minerali e Rocce del C.N.R., P.le A. Moro, 5, I-00185 Roma, Italy

CATERINA DE VITO

Dipartimento di Scienze della Terra, Università degli Studi di Roma “La Sapienza”, P.le A. Moro, 5, I-00185 Roma, Italy

ALEKSANDER ÇINA AND TONIN DEDA

Geological Survey of Albania, Rruga Vasil Shanto, Tirana, Albania

ABSTRACT

The deposit of dawsonite and realgar–orpiment in the Koman area, northern Albania, is aligned along the NE–SW-trending tectonic line joining the Krasta–Cukal and Mirdita structural-tectonic zones. The deposit contains the following main paragenetic assemblages: i) marcasite – greigite (Fe-sulfide stage), ii) stibnite – realgar – orpiment (As–Sb-sulfide stage), iii) dolomite – calcite – dawsonite – aragonite – barite – gypsum (carbonate–sulfate stage), iv) native As – gibbsite (supergene stage). There was lithostratigraphic control of mineralization; carbonate-rich wallrocks reacted with the mineralizing fluids emanating from a buried magmatic body and migrating along Albanian transversal faults, rather than argillaceous lithotypes. Values of $\delta^{18}\text{O}$ and $\delta^{13}\text{C}$ indicate that dawsonite and hydrothermal dolomite are derived at the expense of carbonate rocks, which occur extensively in the stratigraphic sequence of the host rocks. The water:rock ratio during the carbonate–sulfate stage of deposition was probably small. Moreover, oxygen and carbon isotopic exchange during metasomatic transformation of the rocks, recrystallization and late involvement of groundwater, probably all occurred. The sulfur involved in realgar and orpiment deposition may be of magmatic origin, and there was enrichment of heavier S during late hydrothermal processes. Both marcasite and greigite have low Co/Ni values reflecting low-temperature conditions during their formation; the amount of As in the fluids was relatively high during both Fe- and As–Sb-sulfide stages of deposition. The wallrocks were the source of Al and Na involved in dawsonite deposition. Al, Na, K and Si were the elements most effectively leached from rocks during hydrothermal alteration.

Keywords: dawsonite – realgar – orpiment deposit, chemical compositions, stable isotopes, ore genesis, Koman, northern Albania.

SOMMAIRE

Le gisement de dawsonite et de réalgar–orpiment de la région de Koman, dans le nord de l’Albanie, est développé le long de l’axe tectonique NE–SO reliant les zones de Krasta–Cukal et Mirdita. Le gisement contient les assemblages paragénetiques principaux suivants: i) marcasite – greigite (stade des sulfures de fer), ii) stibnite – réalgar – orpiment (stade des sulfures de As–Sb), iii) dolomite – calcite – dawsonite – aragonite – barite – gypse (stade des carbonates–sulfates), iv) As natif – gibbsite (stade supergène). La lithostratigraphie a exercé un contrôle sur la minéralisation; les roches-hôtes carbonatées ont réagi avec les fluides minéralisateurs issus d’un massif magmatique enfoui et migrant le long de failles transversales albanaises plutôt que les roches argilleuses. D’après les valeurs de $\delta^{18}\text{O}$ et de $\delta^{13}\text{C}$, la dawsonite et la dolomite hydrothermale ont été dérivées des roches carbonatées, qui sont répandues dans la séquence stratigraphique de l’encaissant. Le rapport eau:roche au cours du stade des carbonates–sulfates était probablement faible. De plus, il y a eu échange des isotopes de l’oxygène et du carbone au cours de la transformation métasomatique, une recrystallisation et une implication tardive de l’eau des nappes souterraines. Le soufre présent dans la formation du réalgar et de l’orpiment pourrait avoir une origine magmatique, et il y a eu un enrichissement tardif en soufre plus lourd. La marcasite et la greigite possèdent de faibles valeurs de Co/Ni, qui témoignent des conditions de faible température

[§] E-mail address: ferrini@uniroma1.it

lors de leur formation; la quantité d'arsenic dans la phase fluide était relativement élevée lors des stades de déposition des sulfures de fer et de As–Sb. Les roches encaissantes étaient la source de Al et de Na impliqués dans la dawsonite. Ce sont Al, Na, K et Si qui ont été les plus effectivement lessivés des roches lors de l'altération hydrothermale.

(Traduit par la Rédaction)

Mots-clés: gisement de dawsonite – réalgar – orpiment, compositions chimiques, isotopes stables, genèse du minerai, Koman, nord de l'Albanie.

INTRODUCTION

The hydrated carbonate *dawsonite* is considered to be a comparatively rare mineral (e.g., Wopfer & Hocker 1987). Dawsonite was discovered in Montreal, Canada, on the campus of McGill University and the east-southeastern slope of Mont Royal. In its type locality, it occurs as aggregates of acicular to fibrous crystals in the joints of a trachyte dike cutting limestone (Harrington 1874, 1878, Graham 1908, Frueh & Golightly 1967). It also occurs in several sedimentary sequences in various depositional environments: i) associated with eruptive rocks (e.g., Hay 1963, Malesani & Vannucci 1974, Heritsch 1975), ii) not related with magmatic rocks (e.g., De Michele *et al.* 1965, Goldbery & Loughnan 1970), iii) derived but not directly associated with magmatic rocks (Baker *et al.* 1995), and iv) related to hydrothermal mineralization (e.g., Pelloux 1932, Smith & Milton 1966). Koman, in northern Albania, is the only occurrence reported so far of dawsonite in association with realgar and orpiment.

Geological, geochemical and isotopic information about the Koman dawsonite and realgar–orpiment deposit is scarce (e.g., Pelloux 1932, Grazhdani & Bushati 1983). In this paper, we describe the features of the dawsonite, and report on the stable isotope data and major-element composition of the main mineralogical phases and carbonate-bearing wallrocks associated with the mineralization. An attempt is made to define the main processes that contributed to the formation of the deposit.

GEOLOGY AND MINERALIZATION

Main geology

The dawsonite and realgar–orpiment deposit in the Koman area (Fig. 1) is located along the course of the river Drin, about 15 km north of the town of Puka. The occurrences are aligned along the NE–SW-trending tectonic line joining the Krasta–Cukal (footwall) and Mirdita (hanging-wall) structural-tectonic zone (Grazhdani 1987, Grazhdani *et al.* 1989).

The Mirdita zone, near the deposit, consists of Triassic limestone with lenses of chert, argillaceous schist, sandstone and volcanic rocks, ultramafic rocks (Jurassic), and the volcano-sedimentary series of the Mirdita

ophiolitic complex (Triassic–Jurassic). The Eastern Ophiolitic Belt of Mirdita is well known in the literature, as it hosts many chromite deposits, representing one of the most important mineral commodities of Albania.

The Krasta–Cukal zone, also near the deposit, consists of a sequence of terranes composed of cherty limestone and radiolarite (Jurassic to Lower Cretaceous), limestone (Upper Cretaceous) and carbonate schist, sandstone and conglomerate (“Xhan Flysch”, Upper Cretaceous to Lower-Middle Paleogene). Granitic rocks are particularly widespread in the Levrushku (Jurassic? Cretaceous?) and Fierza–Poravi areas (Middle Jurassic), about 25 km northeast of Koman (Xhomo *et al.* 2002). These terranes define an anticlinorium with a southward dip.

The occurrences of dawsonite and realgar–orpiment studied here outcrop mainly near the Shkodra–Pec regional alignment (Fig. 1), being deposited mainly within the marlstone, argillaceous schist, carbonate and sandstone of the Xhan Flysch of the Krasta–Cukal area, and subordinately within Triassic argillaceous schists of the Mirdita zone. The mineralized area has a NE–SW to E–W trend with a 60–70° dip ranging from southeast to south. At Dushman, about 10 km northeast of Koman, in the vicinity of the mineralized area, volcanic rocks (mainly dacite–andesite) also are exposed; these rocks occur as olistoliths of Middle Triassic age in the Paleogene flysch.

The deposits of dawsonite and realgar–orpiment preferentially lie within carbonate-rich layers up to 30–50 cm thick, in some cases cutting across cleavage surfaces, and outcrop in a belt of about 3 × 0.5 km by 300 m thick. The dawsonite-rich horizon is 500 × 100 m by 20 m thick (Leka *et al.* 1997). The estimated potential reserves of dawsonite are 2 × 10⁶ tonnes at 10–15% average grade in the carbonate wallrocks, and 5 × 10⁶ tonnes at 5% average grade in the sandstone occurring in the Xhan Flysch formation (Borova *et al.* 1991). These occurrences were deposited mainly between argillaceous schists and the marlstone – argillaceous schist – carbonate – sandstone formation, and show two main forms: i) dawsonite associated with realgar–orpiment, and ii) dawsonite as the only ore mineral.

In the Dinarides, it is worth noting that the main As–Sb–Tl–Au mineralization is the Alšar deposit (Jankovic *et al.* 1997) in the Kozuf district (former Yugoslav Re-

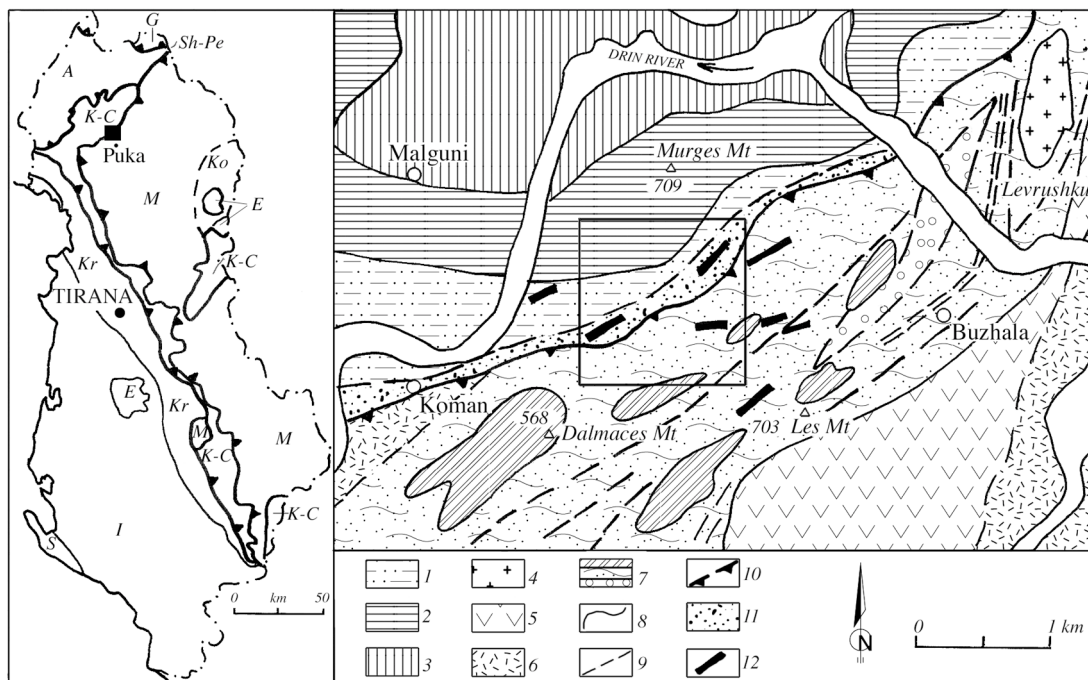


FIG. 1. Geological sketch-map of the Koman region. Krasta–Cukal zone: 1) Xhan Flysch (Upper Cretaceous – Lower-Middle Paleogene), 2) limestone (Upper Cretaceous), 3) cherty limestone (Upper Jurassic – Lower Cretaceous); Mirdita zone: 4) granite (Jurassic? Cretaceous?), 5) volcano-sedimentary series (Triassic–Jurassic), 6) ophiolitic formation (Jurassic), 7) limestone and argillaceous schists with lenses of silexite (Triassic); 8) stratigraphic boundaries; 9) faults; 10) overthrusts; 11) zone of realgar–orpiment and dawsonite mineralization; 12) mineralized bodies. Square: area of Figure 5. Inset: tectonic sketch-map of Albania (simplified from Shallo *et al.* 1985) showing location (black rectangle) of study area. Tectonic zones: Ko: Korrab; G: Gash; M: Mirdita; K–C: Krasta–Cukal; Kr: Kruja; I: Ionian; S: Sazan; E: evaporite diapirs; A: Alps. Sh–Pe: Shkodra–Pec tectonic alignment.

public of Macedonia, about 120 km southeast of Koman), whereas the main polymetallic mineralization is the Trepça deposit in the Kopaonik Massif (Serbia, about 100 km northeast of Koman). These examples of mesothermal to epithermal mineralization are closely linked with local acidic to intermediate-acidic Tertiary magmatism. Other realgar–orpiment deposits in the Albanides (Hoxha 2001) have been discovered at Radomira, Stanet, Preshit, Dipjaka and Bardhe, in the Korrab Mountains, about 70 km southeast of Koman, in eastern Albania. None of these deposits contain dawsonite.

Minor occurrences of Hg, barite and Pb–Zn–Ba were found in the Cukal region, and at Qerret and Levrushku, further south (Hoxha 2001).

Petrography of the wallrocks

The wallrocks of the dawsonite occurrence mainly consist of dolostone, principally composed of microcrystalline dolomite and ankerite, with subordinate

amounts of quartz and clay minerals, which form microscopic laminae, causing in places a slightly oriented fabric in the rock. Realgar, orpiment, dawsonite and marcasite also occur as disseminations, vugs, small pockets, and veinlets along cleavage planes of the dolostone or in transversal fractures. In the latter case, opaque minerals are also associated with quartz, and dolostone in places shows slight recrystallization of dolomite, cemented by calcite.

Mineralization has also affected sandstone and shale, and to a lesser extent, argillaceous rocks and schist formations. The sandstone is composed of abundant quartz, feldspar and scarce calcitic cement, whereas the shale consists of very fine quartz and very thin K-mica and clay crystals oriented in the direction of bedding. In both rocks, the replacement of a primary calcareous mudstone matrix containing planctonic microfossils was observed. The sandstone and shale host only subordinate amounts of dawsonite and associated hydrothermal mineral phases, forming veinlets cutting across the wallrocks.

Mineralogy

In order of decreasing abundance, the mineralized bodies contain dawsonite, realgar and orpiment, with subordinate marcasite, greigite and occasional stibnite, and as gangue minerals, mainly dolomite, quartz (also chalcedony), with subordinate calcite, aragonite, barite and gypsum. Native As, gibbsite, arsenolite, pharmacolite and goethite occur as supergene minerals.

Dawsonite occurs as veinlets and nodular aggregates, generally associated with early-deposited realgar, orpiment and quartz within limestone, and shows an acicular, radially concentric texture (Fig. 2). It also occurs as tabular crystals and radially concentric aggregates inside rhombs of dolomite and calcite. Gibbsite is closely associated with the dawsonite.

Realgar also occurs as veinlets and nodules within dolostone, marlstone, sandstone and limestone. Near occurrences of realgar, the dolostone is generally recrystallized to a larger grain-size (Fig. 2). Moreover, veins of diagenetic calcite are replaced or cemented by realgar, and nodular aggregates of realgar and calcite may be found within some quartz veinlets.

Orpiment usually occurs in association with realgar, in aggregates cementing the largest crystals of dolomite, where the latter occurs in veins. The prismatic crystals of orpiment also penetrate the largest crystals of dolomite, replacing them. Textural relationships reveal that the aggregates of realgar are surrounded by idiomorphic crystals of orpiment, but may also include them; orpiment is also due to the pseudomorphic transformation of realgar (Fig. 2).

Accessory minerals are stibnite, as elongate crystals within realgar (Fig. 3), marcasite, greigite and native As. Greigite, an epithermal mineral, occurs as a primary

phase in the Koman deposit and, with marcasite, forms i) round and tabular aggregates and nodules with banded, concentric, spheroidal (Fig. 3) and fibroradial textures, disseminated within wallrocks, ii) crystals within realgar–orpiment (Fig. 4), and iii) small lenses inside dawsonite. The occurrence of stibnite and greigite in this deposit had not been reported.

SAMPLING AND ANALYTICAL PROCEDURE

The samples we collected are representative of limestone, marlstone and argillaceous rocks within the Upper Cretaceous to Lower-Middle Paleogene flysch, and of the main mineral phases. A first group of wallrock samples was collected at an average interval of 50–200 m (total length about 1 km) along a NW–SE cross-section (A–A in Fig. 5) in the mineralized area; a second group was collected in a layer of dolostone relatively enriched in dawsonite and arsenic minerals. Particular attention was paid to these carbonate rocks, the most greatly affected by hydrothermal fluids.

Prior to chemical and isotopic investigations, all samples were examined in polished thin section to establish mineral assemblages and textures. Confirmation of the presence of the mineral phases recognized was made with a Seifert automatic X-ray powder diffractometer (accelerating voltage 15 kV, beam current 30 mA, Ni-filtered Cu radiation, graphite monochromator, 2θ step 0.02°).

Selected samples of the various types of wallrocks were analyzed by X-ray fluorescence and atomic absorption spectroscopy after determination of H₂O⁻ and LOI. Determination of major-element contents of the main mineral phases was carried out by electron-microprobe analysis (Cameca Camebax Microbeam, equipped

TABLE 1. COMPOSITION OF THE WALLROCKS OF THE KOMAN DEPOSIT, ALBANIA

	KO-1-u	KO-11-u	mean	s.d.	KO-8-n	KO-2-u	KO-12-u	mean	s.d.	KO-6-n		KO-3-u	KO-4-u	KO-10-u	mean	s.d.	KO-5-n	KO-7-n	KO-9-n	mean	s.d.
	ls	ls			ls	marl.	marl.			marl.		arg.	arg.	arg.			arg.	arg.	arg.		
SiO ₂ wt.%	5.87	2.03	3.95	2.72	8.71	34.93	32.67	33.8	1.6	28.88		39.48	53.36	53.12	48.65	7.95	54.3	47.46	56.88	52.88	4.87
Fe ₂ O ₃	0.94	0.4	0.67	0.38	0.97	4.32	4.4	4.36	0.06	3.1		7.54	8.19	2.91	6.21	2.88	4.52	7.39	7.0	6.3	1.56
TiO ₂	n.d.	n.d.			n.d.	0.4	0.4	0.4	0	0.33		0.56	0.96	0.33	0.62	0.32	0.48	0.69	0.87	0.68	0.2
Al ₂ O ₃	2.2	1.32	1.76	0.62	2.02	9.68	6.53	8.11	2.23	5.12		12.73	17.99	5.46	12.06	6.29	9.15	14.26	14.3	12.57	2.96
CaO	50.02	53.24	51.63	2.28	47.59	23.72	27.13	25.43	2.41	29.44		11.89	2.64	19.76	11.43	8.57	13.36	7.51	5.71	8.86	4.0
MgO	0.04	0.42	0.23	0.27	0.95	2.6	2.09	2.35	0.36	3.26		4.92	4.44	1.15	3.5	2.05	2.28	4.16	3.18	3.21	0.94
Na ₂ O	0.34	0.12	0.23	0.16	0.47	0.83	0.77	0.8	0.04	1.25		1.29	1.42	0.96	1.22	0.24	1.33	1.33	1.16	1.27	0.1
K ₂ O	0.31	0.22	0.27	0.06	0.16	1.65	0.78	1.22	0.62	0.5		2.06	3.73	0.5	2.1	1.62	1.19	3.0	3.2	2.46	1.11
H ₂ O ⁻	0.06	0.12	0.09	0.04	0.17	0.3	0.55	0.43	0.18	0.52		0.4	0.64	0.12	0.39	0.26	0.29	0.54	0.45	0.43	0.13
LOI	39.66	41.56	40.61	1.34	38.52	21.05	25.0	23.03	2.79	27.07		18.27	6.44	15.97	13.56	6.27	12.22	12.9	7.15	10.76	3.14
Total	99.44	99.43			99.56	99.48	100.32			99.47		99.14	99.81	100.28			99.12	99.24	99.9		
Na/K	0.98	0.49	0.73	0.35	2.63	0.45	0.88	0.67	0.31	2.23		0.56	0.34	1.72	0.87	0.74	1.0	0.4	0.32	0.57	0.37

Symbols: ls: limestone, marl.: marlstone, arg.: argillaceous rocks; s.d.: standard deviation, n.d.: not detected, u: unmineralized, n: near mineralization.

TABLE 2. ELECTRON-MICROPROBE DATA ON MAIN MINERAL PHASES PRESENT IN THE KOMAN DEPOSIT, ALBANIA

Dawsonite					Dolomite (wallrock)				
ideal: 35.4% Al ₂ O ₃ , 21.5% Na ₂ O, 30.6% CO ₂ , 12.5% H ₂ O					ideal: 30.4% CaO, 21.9% MgO, 47.7% CO ₂				
	mean	± s.d.	n/6	e		mean	± s.d.	n/13	e
Al ₂ O ₃	47.15	± 2.17	6	0.05	CaO	32.12	± 1.33	13	0.05
Na ₂ O	10.38	± 1.35	6	0.04	MgO	19.52	± 1.23	13	0.06
CaO	0.36	± 0.15	6	0.06	FeO	0.82	± 0.55	12	0.05
MgO	0.26	± 0.08	2	0.05	MnO	0.38	± 0.30	11	0.05
K ₂ O	0.14	± 0.07	2	0.06	Na ₂ O	0.28	± 0.06	10	0.04
As ₂ O ₃	1.47	± 0.43	3	0.09	K ₂ O	0.15	± 0.02	8	0.06
SO ₃	0.20	± 0.10	6	0.06	Al ₂ O ₃	1.28	± 0.46	11	0.06
CO ₂	31.57	± 1.58	6	2.10	SiO ₂	1.17	± 0.45	10	0.05
H ₂ O	9.21	± 3.75	6		CO ₂	45.88	± 1.58	13	
Dolomite (hydrothermal)					Ankerite (wallrocks)				
ideal: 30.4% CaO, 21.9% MgO, 47.7% CO ₂					ideal: 28.0% CaO, 10.0% MgO, 18.0% FeO, 44.0% CO ₂				
	mean	± s.d.	n/10	e		mean	± s.d.	n/12	e
CaO	33.18	± 0.12	10	0.04	CaO	30.60	± 0.94	12	0.06
MgO	19.43	± 0.88	10	0.06	MgO	13.22	± 1.01	12	0.05
FeO	1.30	± 0.36	7	0.05	FeO	9.64	± 2.60	12	0.04
MnO	0.55	± 0.35	7	0.06	MnO	0.53	± 0.40	11	0.05
Na ₂ O	0.28	± 0.14	10	0.04	Na ₂ O	0.26	± 0.29	10	0.04
Al ₂ O ₃	0.75	± 0.34	9	0.06	Al ₂ O ₃	0.51	± 0.19	11	0.06
CO ₂	45.21	± 0.26	10		P ₂ O ₅	0.45	± 0.06	10	0.05
					CO ₂	45.27	± 0.39	13	
Calcite (hydrothermal)					Stibnite				
ideal: 56.0% CaO, 44.0% CO ₂					ideal: 71.7% Sb, 28.3% S				
	mean	± s.d.	n/8	e		mean	± s.d.	n/10	e
CaO	54.77	± 1.14	8	0.05	Sb	65.59	± 0.87	10	0.13
MnO	1.22	± 1.00	8	0.06	As	5.02	± 0.55	10	0.11
MgO	0.36	± 0.10	6	0.05	Se	0.18	± 0.08	2	0.09
FeO	0.72	± 0.06	5	0.07	S	28.76	± 0.20	10	0.12
CO ₂	43.19	± 0.27	8						
Orpiment					Realgar				
ideal: 60.9% As, 39.1% S					ideal: 70.0% As, 30.0% S				
	mean	± s.d.	n/5	e		mean	± s.d.	n/16	e
As	57.75	± 1.45	5	0.12	As	68.01	± 0.61	16	0.12
Sb	1.62	± 0.09	5	0.14	Se	0.58	± 0.02	16	0.09
Se	0.53	± 0.06	5	0.11	S	31.78	± 0.59	16	0.10
Hg	0.12	± 0.01	2	0.06					
Zn	0.17	± 0.03	2	0.08					
S	40.12	± 0.68	5	0.12					
Marcasite					Greigite				
ideal: 53.5% S, 46.5% Fe					ideal: 46.4% S, 56.6% Fe				
	mean	± s.d.	n/7	e		mean	± s.d.	n/7	e
Fe	44.64	± 0.72	7	0.06	Fe	55.15	± 3.32	7	0.07
Ni	2.15	± 0.09	2	0.07	Ni	0.32	± 0.04	7	0.06
Co	0.72	± 0.07	2	0.06	As	0.71	± 0.59	3	0.09
As	0.60	± 0.09	7	0.11	S	42.36	± 2.34	7	0.10
S	52.20	± 0.23	7	0.12					

Note: e is the standard error, expressed as a percentage.

with three wavelength-dispersion spectrometers operating at an accelerating voltage of 15 kV and a beam current of 30 nA, with an acquisition time of 10 s on both peak and background; data reduction with ZAF correction software). We used natural and synthetic standards: diopside (SiK α , CaK α , MgK α lines), corundum (AlK α), albite (NaK α), orthoclase (KK α), synthetic diamond (CK α), fayalite (FeK α), apatite (PK α), pyrite (SK α , FeK α), sphalerite (ZnK α), arsenopyrite (AsL α), synthetic HgSe (HgM α , SeL α), metallic Mn, Ni, Co (K α) and Sb (L α).

The $\delta^{18}\text{O}$, $\delta^{13}\text{C}$ and $\delta^{34}\text{S}$ of selected concentrates of quartz, dawsonite, dolomite, realgar, orpiment (purity checked by XRD, >98%) and carbonate rocks were obtained by conventional mass spectrometry (reaction under vacuum of selected mineral phases with orthophosphoric acid to extract O and C from carbonates, hydrofluoric acid to extract O from quartz, and nitric acid to extract S from As sulfides) and expressed as $\delta^{18}\text{O}$, $\delta^{13}\text{C}$ and $\delta^{34}\text{S}$ (replicate error of initial value $\leq \pm 0.20$, ± 0.10 and $\pm 0.20\%$, respectively) against SMOW, PDB and CDT standards.

EXPERIMENTAL RESULTS

Tables 1 and 2 show major-element contents of wallrocks and the main mineral phases, respectively. Table 3 lists the bulk chemical composition of the dawsonite ore. The $\delta^{18}\text{O}$, $\delta^{13}\text{C}$ and $\delta^{34}\text{S}$ of quartz, dawsonite, dolomite, realgar, orpiment separates and carbonate rocks are shown in Table 4. The data and mean calculations reported in this work are representative of replicate analyses carried out on several samples.

Petrography of wallrocks

The limestone and marlstone near the mineral occurrence have higher Na contents than the corresponding unmineralized rocks. The mean Na/K values of the two corresponding categories are as follows: limestone 2.63 and 0.73 \pm 0.35, marlstone 2.23 and 0.67 \pm 0.31, argillaceous rocks 0.87 \pm 0.74 and 0.57 \pm 0.37, respectively (Table 1). Na/K values are in any case also very small in comparison with those (10–50) of wallrocks in other occurrences of dawsonite in various geological contexts in the world (Hay 1964).

A plot of wallrock compositions in terms of the (Na₂O + K₂O) – Al₂O₃ – SiO₂ diagram (Fig. 6) shows that samples near the mineralized zone fall within a narrow field included in that of unmineralized samples. Slight recrystallization by mineralized fluids thus led to a greater chemical “homogeneity” of the resulting rock.

With regards to the main mineralogical constituents of wallrocks of the dawsonite occurrence, dolomite and ankerite also contain subordinate Mn (\bar{x} = 0.38 and 0.53% MnO, respectively), Na (\bar{x} = 0.28 and 0.26% Na₂O) and Al (\bar{x} = 1.28 and 0.51% Al₂O₃). In addition, the dawsonite contains Fe, Si and K (\bar{x} = 0.82, 1.17 and

0.15% of the respective oxides), whereas ankerite hosts P ($\bar{x} = 0.45\%$ P_2O_5). A high standard deviation from mean values reflects differences in composition among the single grains of both dolomite and ankerite from wallrocks.

Mineralogy

The dawsonite contains more Al ($\bar{x} = 47.15\%$ Al_2O_3), slightly more CO_2 ($\bar{x} = 31.57\%$) and, conversely, less Na ($\bar{x} = 10.38\%$ Na_2O) and slightly less H_2O ($\bar{x} = 9.21\%$) with respect to the theoretical composition; bulk compositions of the dawsonite ore confirm these differences. This result contrasts with a single composition reported by Pelloux (1932), in which dawsonite was described as being nearly stoichiometric. The EPM analyses carried out on the samples studied invariably display the observed high Al content, and confirm its peculiar composition. Moreover, the dawsonite contains subordinate Ca ($\bar{x} = 0.36\%$ CaO), Mg ($\bar{x} = 0.26\%$ MgO), K ($\bar{x} = 0.14\%$ K_2O), As ($\bar{x} = 1.47\%$ As_2O_3), and SO_3 ($\bar{x} = 0.20\%$).

Both marcasite and greigite have higher contents of Ni with respect to Co ($\bar{x} = 2.15$ and 0.72% ; 0.32% and below detection limit, respectively) and relatively high As contents ($\bar{x} = 0.60$ and 0.71% , respectively).

Realgar shows no significant differences with respect to the stoichiometric formula, whereas in

orpiment, there is substitution of Sb for As ($\bar{x} = 1.62\%$) and subordinate contents of Hg ($\bar{x} = 0.12\%$) and Zn ($\bar{x} = 0.17\%$). In stibnite, there is substitution of Sb for As ($\bar{x} = 5.02\%$). Realgar, orpiment and stibnite have significant Se contents ($\bar{x} = 0.58, 0.53$ and 0.18% , respectively).

Stable isotope data

The unrecrystallized and slightly recrystallized dolostones have $\delta^{18}\text{O} = 39.92 \pm 1.4\%$ and $38.8 \pm 0.7\%$ and $\delta^{13}\text{C} = 4.7 \pm 0.7\%$ and $1.4 \pm 0.3\%$, respectively (Table 4). The $\delta^{18}\text{O}$ values are high compared with those of sedimentary carbonates ($10 < \delta^{18}\text{O} < 35\%$: Veizer & Hoefs 1976, Faure 1986, Schroll 1984), particularly with those of marine limestone and remobilized carbonates in the world ($28 < \delta^{18}\text{O} < 30\%$: Faure 1986), whereas the $\delta^{13}\text{C}$ values fit the range reported in the literature ($\delta^{13}\text{C} > 0\%$: Veizer & Hoefs 1976, Schroll 1984, Faure 1986; $-10 < \delta^{13}\text{C} < +8\%$: Ohmoto & Rye 1979; unaltered marine carbonate: $-2.5 < \delta^{13}\text{C} < +2.5\%$: Ripperdan 2001).

The $\delta^{18}\text{O}$ of the selected minerals show a range of values: dawsonite ($\bar{x} = 43.3 \pm 0.6\%$), hydrothermal dolomite ($\bar{x} = 39.4 \pm 0.2\%$) and quartz ($\bar{x} = 2.7 \pm 0.3\%$). The $\delta^{13}\text{C}$ values of hydrothermal dolomite ($\bar{x} = 6.4 \pm 0.4\%$) and dawsonite ($\bar{x} = 5.9 \pm 0.2\%$) show less marked differences. As previously noted regarding

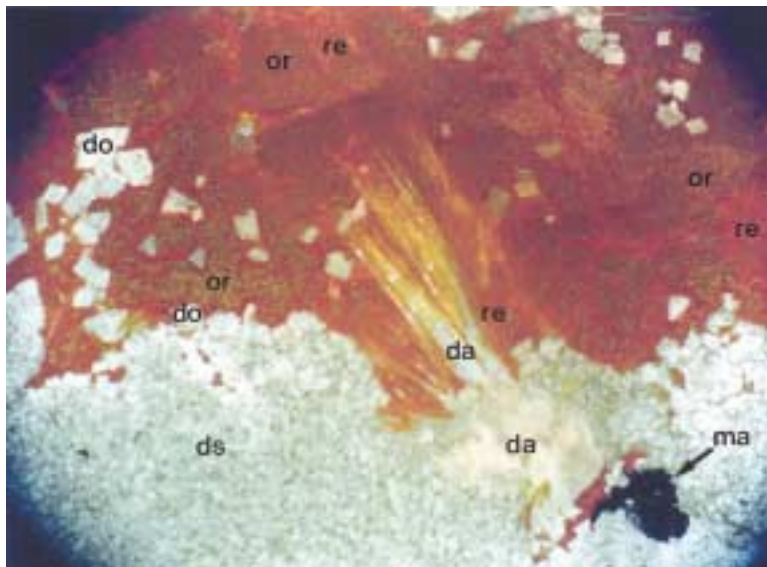


FIG. 2. Photomicrograph showing textural relationships among acicular, radially concentric and nodular dawsonite (da) replacing realgar (re), in places transformed into orpiment (or), marcasite (ma) and recrystallized dolomite (do), deposited in dolostone (ds) of the Koman deposit (reflected light, crossed nicols, $50\times$).

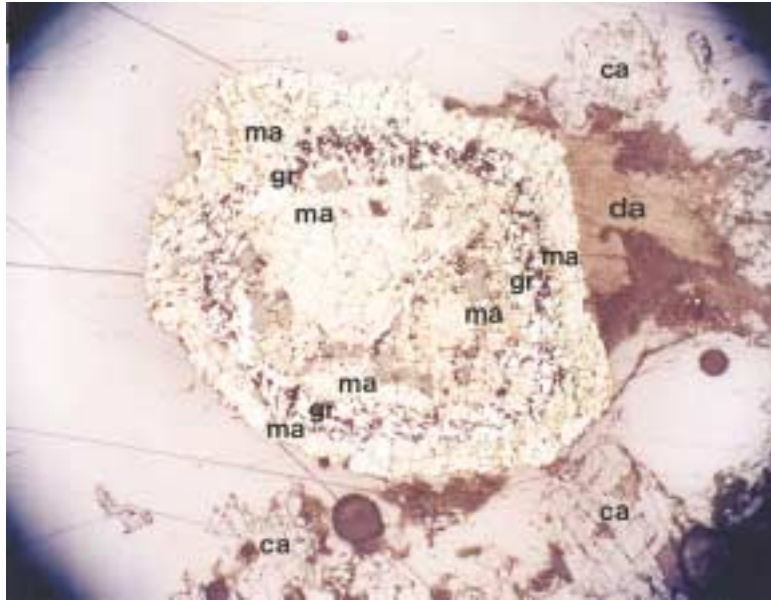


FIG. 3. Photomicrograph showing marcasite (ma) and greigite (gr) with spheroidal concentric texture, dawsonite (da) and calcite (ca) in the Koman deposit (reflected light, parallel nicols, 50 \times).

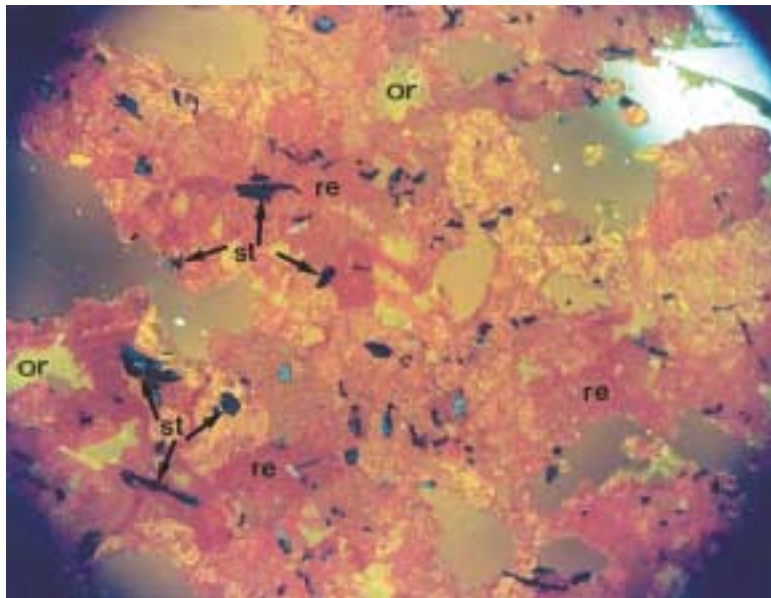


FIG. 4. Photomicrograph showing textural relationships among realgar (re), orpiment (or) and stibnite (st) in ore sample from the Koman deposit (reflected light, crossed nicols, 50 \times).

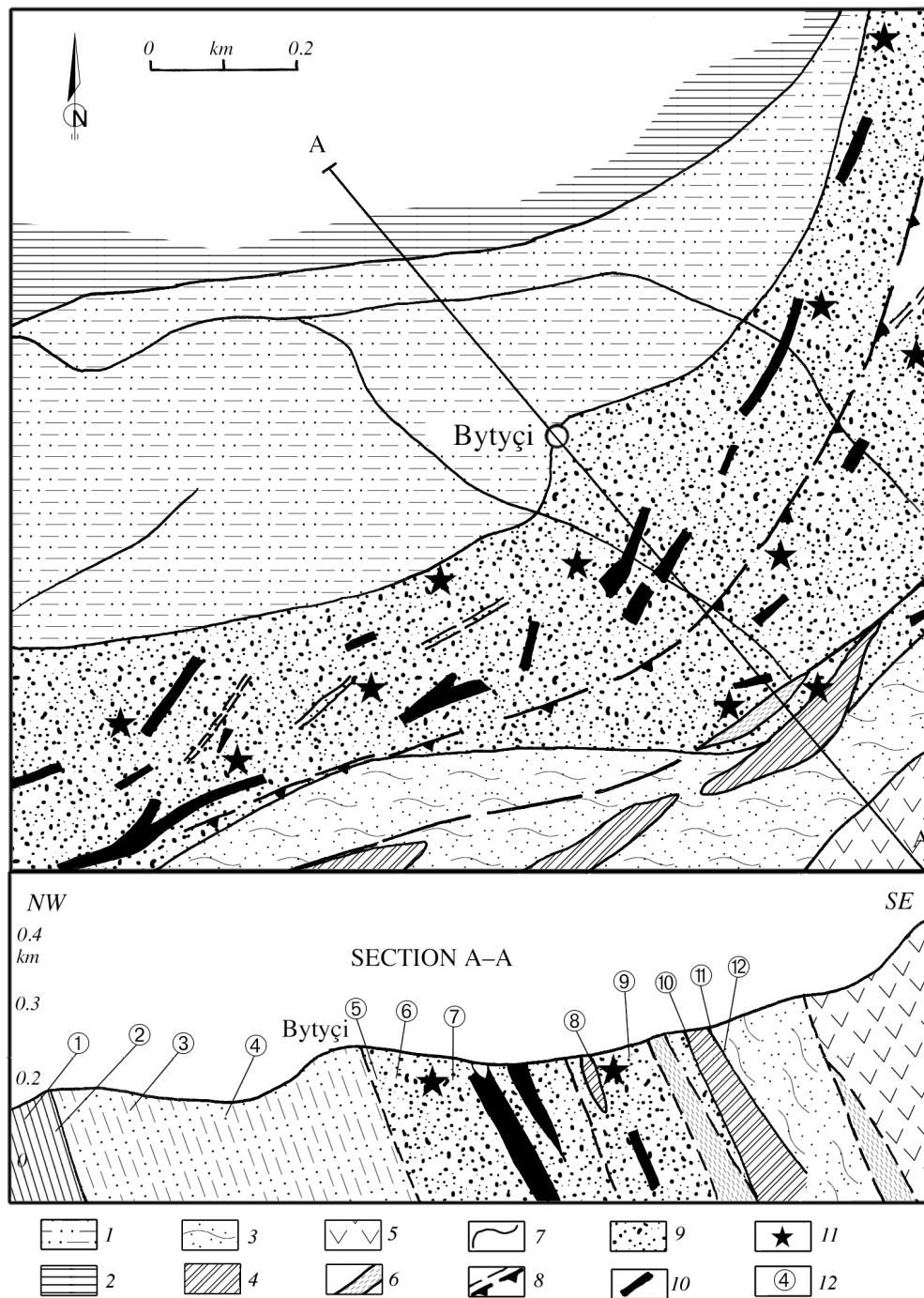


FIG. 5. Geological sketch-map and representative cross-section (A-A) through local stratigraphic succession of the Koman mineralized area. Krasta-Cukal zone: 1) marlstone – argillaceous schist – carbonate – sandstone formations of Xhan Flysch (Upper Cretaceous – Lower-Middle Paleogene), 2) limestone (Upper Cretaceous). Mirdita zone: 3) argillaceous schists (Triassic), 4) limestone (Triassic), 5) volcano-sedimentary series (Triassic–Jurassic), 6) ophiolitic serpentinite, 7) stratigraphic boundaries, 8) faults and overthrusts, 9) mineralized zone, 10) realgar–orpiment occurrences, 11) dawsonite occurrences, 12) sample numbers in section A–A (reported as KO–1 to KO–12 in Table 1).

dolostone, the $\delta^{18}\text{O}$ values of carbonate minerals are also slightly higher than the maximum values of the range of other sedimentary carbonates in general, and of recent marine limestone, whereas $\delta^{13}\text{C}$ are in good agreement with those ranges.

Quartz has a mean $\delta^{18}\text{O}$ value of $2.7 \pm 0.3\text{‰}$, which fits the range of ore fluids associated with some epithermal deposits ($-15 < \delta^{18}\text{O} < 9\text{‰}$; O'Neil & Silberman 1974, Casadevall & Ohmoto 1977, Kamilli & Ohmoto 1977, Hattori & Sakai 1979, O'Neil & Bailey 1979, Radtke *et al.* 1980, Robinson & Christie 1980).

Unfortunately, there are few isotopic data on dawsonite and associated mineral phases in the literature ($9.8 < \delta^{18}\text{O} < 37.6\text{‰}$ and $-4 < \delta^{13}\text{C} < +4.8\text{‰}$; Boussarouque *et al.* 1975, Baker *et al.* 1995). The isotopic composition of the Koman dawsonite shows high values of oxygen and carbon isotopes when compared with those data in the literature. In fact, in the $\delta^{18}\text{O}$ versus $\delta^{13}\text{C}$ diagram (Fig. 7), our samples plot beyond the field of oxygen and carbon isotope values characterizing dawsonite that is linked to hydrothermal and volcanic processes (Boussarouque *et al.* 1975, Baker *et al.* 1995). In the same diagram, we also plot the values for dolostone and hydrothermal dolomite.

The $\delta^{34}\text{S}$ values of realgar and orpiment have a narrow range ($\bar{x} = 6.5 \pm 0.7$ and $7.1 \pm 0.3\text{‰}$, respectively).

DISCUSSION

Textural relationships and microscopic features allow us to define the following main paragenetic assemblages (Fig. 8): marcasite and greigite were the first

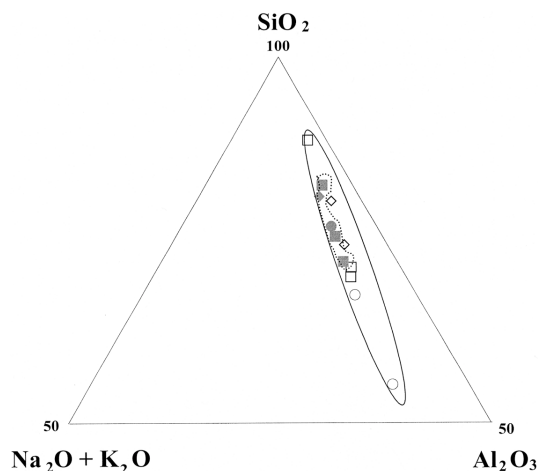


FIG. 6. $(\text{Na}_2\text{O} + \text{K}_2\text{O}) - \text{Al}_2\text{O}_3 - \text{SiO}_2$ diagram for wallrocks of the Koman deposit. Dotted and solid lines, and full and open symbols, refer to samples near mineralized and unmineralized rocks, respectively. Symbols: ●○: limestone, ◆◇: marlstone, and ■□ argillaceous rock.

TABLE 3. RANGE OF CHEMICAL COMPOSITION OF DAWSONITE ORE, KOMAN DEPOSIT

Al ₂ O ₃ , wt.%	30 - 37	according to stoichiometry:	35.4
Na ₂ O	15 - 21		21.5
CO ₂	35 - 37		30.6
H ₂ O ⁺	4		12.5
H ₂ O ⁻	0.5 - 1		

TABLE 4. VALUES OF $\delta^{18}\text{O}$, $\delta^{13}\text{C}$ and $\delta^{34}\text{S}$ FOR SELECTED MINERALS AND WALLROCKS, KOMAN DEPOSIT, ALBANIA

		$\delta^{18}\text{O}$ ‰	$\delta^{13}\text{C}$ ‰	$\delta^{34}\text{S}$ ‰
Mineral phases				
KO-1Qz	quartz	2.7	—	—
KO-2Qz	quartz	2.9	—	—
KO-3Qz	quartz	3.0	—	—
KO-4Qz	quartz	2.4	—	—
mean		2.7		
s.d.		0.3		
KO-1D	dawsonite	43.7	5.7	—
KO-2D	dawsonite	43.9	5.6	—
KO-3D	dawsonite	42.5	6.2	—
KO-4D	dawsonite	43.0	5.9	—
KO-5D	dawsonite	43.6	6.1	—
KO-6D	dawsonite	42.8	6.0	—
mean		43.3	5.9	
s.d.		0.6	0.2	
KO-1DD	dolomite	39.4	6.4	—
KO-2DD	dolomite	39.5	5.9	—
KO-3DD	dolomite	39.6	6.2	—
KO-4DD	dolomite	39.1	6.9	—
mean		39.4	6.4	
s.d.		0.2	0.4	
KO-1R	realgar	—	—	6.0
KO-2R	realgar	—	—	7.1
KO-3R	realgar	—	—	5.8
KO-4R	realgar	—	—	7.0
mean				6.5
s.d.				0.7
KO-1O	orpiment	—	—	7.1
KO-2O	orpiment	—	—	7.3
KO-3O	orpiment	—	—	6.8
mean				7.1
s.d.				0.3
Wallrocks				
KO-1Ds	dolostone (unrecrystallized)	41.3	5.4	
KO-2Ds	dolostone (unrecrystallized)	39.5	5.1	
KO-3Ds	dolostone (unrecrystallized)	39.8	4.2	
KO-4Ds	dolostone (unrecrystallized)	37.9	3.9	
KO-5Ds	dolostone (slightly recrystall.)	39.7	1.5	
KO-6Ds	dolostone (slightly recrystall.)	38.8	1.8	
KO-7Ds	dolostone (slightly recrystall.)	38.2	1.5	
KO-8Ds	dolostone (slightly recrystall.)	39.3	1.1	
KO-9Ds	dolostone (slightly recrystall.)	37.9	1.3	
mean		39.2	2.9	
s.d.		1.1	1.8	
unrecrystallized, mean		39.6	4.7	
s.d.		1.4	0.7	
slightly recrystallized, mean		38.8	1.4	
s.d.		0.7	0.3	

Note: s.d.: standard deviation.

minerals to be deposited by mineralizing fluids (Fe-sulfide stage). They were followed by quartz and rare stibnite and, in turn, by realgar and orpiment, accompanied by calcite (As–Sb-sulfide stage). Then, dolomite and calcite recrystallized, after which dawsonite was deposited, accompanied by rare aragonite, barite and gypsum (carbonate–sulfate stage). During a late stage, native As and gibbsite formed at the expense of realgar–orpiment and dawsonite, respectively. Lastly, arsenolite, pharmacolite and goethite were deposited at the supergene stage.

The low concentration of dawsonite and associated hydrothermal mineral phases in the sandstone and shale occurring within the argillaceous and schist wallrocks, compared to the grade in the carbonate rocks, is probably due to its lower permeability, porosity and density of fractures, and to its lower reactivity, and thus tendency to replacement. There is thus a strong local lithostratigraphic control by carbonate rocks, which show a very high reactivity with the hydrothermal fluids.

On the basis of comparisons between mineralized and unmineralized rocks (Table 1, Fig. 6), we note that

Al, Na, K and Si are the elements most effectively mobilized during hydrothermal alteration of wallrocks. The similar mean and high standard deviation values between mineralized and unmineralized argillaceous rocks are due to their relative lack of reactivity and thus, inability to host mineralization.

Moreover, with regard to major-element contents, wallrock and hydrothermal dolomite have similar mean values, showing that hydrothermal dolomite probably was derived by the leaching of dolomite from wallrocks by hydrothermal solutions. In terms of minor-element contents, the lack of K and Si in the hydrothermal dolomite could be ascribed to high dilution with respect to these elements in the late fluids (Table 2).

In order to interpret the isotopic compositions of the carbonate minerals at Koman, we modeled our data supposing a hydrothermal system interacting with carbonate-rich host rocks. In these conditions, the isotopic compositions are the result of isotopic re-equilibration between hydrothermal fluids and the wallrocks.

As dolomite and dawsonite have $\delta^{18}\text{O}$ values comparable with those of the wallrock dolostone, we do not

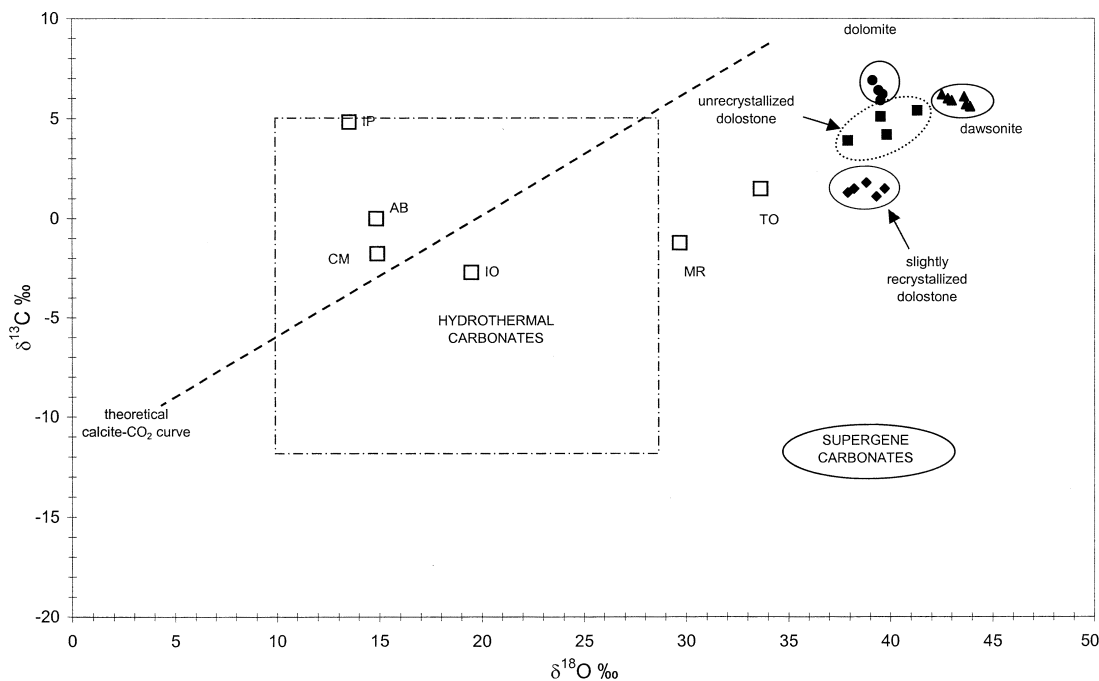


FIG. 7. C and O isotope composition of carbonate minerals and rocks of the Koman deposit, expressed as $\delta^{13}\text{C}$ and $\delta^{18}\text{O}$ values. Also shown: theoretical calcite– CO_2 curve (dotted line, Robinson 1974), field of supergene carbonates (ellipse, Robinson 1974), and reference field for carbonate minerals and rocks from other examples of hydrothermal mineralization (rectangle; Schroll 1984, Robinson 1974, Rye & Ohmoto 1974). TO: Tanzania, Olduvai Gorge, low-temperature encrustation; MR: Mauritania, Richât, both low-temperature – hydrothermal; IO: Italy, Orciatico, hydrothermal; CM: Canada, McGill University campus, hydrothermal; IP: Italy, Piancastagnaio, hydrothermal (Boussaroque *et al.* 1975); AB: Australia, Bowen – Gunnedah – Sydney, deep seepage circulation at moderate temperature (Baker *et al.* 1995).

consider likely the possibility that oxygen isotope disequilibrium (Cole 1994, 2000, Cole & Chakraborty 2001), observed in many low-temperature ($T < 200^{\circ}\text{C}$) hydrothermal ore deposits, gave rise to the high $\delta^{18}\text{O}$ values at Koman.

The high mean $\delta^{18}\text{O}$ values of the unrecrystallized and slightly recrystallized dolostones at Koman fit the hypothesis of Ohmoto & Rye (1979) about the high values of these parameters in dolomitized carbonate rocks. The process of dolomitization of the wallrock probably caused a relative enrichment in heavier oxygen (*e.g.*, O'Neil & Epstein 1966, Sheppard & Schwarz 1970, Tan & Hudson 1971) in comparison with marine limestone, the probable precursor.

Comparing the isotopic compositions of both types of dolostone, we observe that hydrothermal crystallization typically causes a lowering of $\delta^{13}\text{C}$ and no significant differences in $\delta^{18}\text{O}$ (Fig. 7). Thus, isotopic exchange took place, with recrystallization of the rock, as usually observed in other hydrothermally altered carbonate areas (Sverjensky 1981). This difference in $\delta^{13}\text{C}$, about 3‰, is relatively small and may be directly re-

lated, at previously inferred temperatures of $<75\text{--}85^{\circ}\text{C}$ for the carbonate stage, to the water:rock ratio which, consequently, should be small (Sverjensky 1981). Alternatively, these fluids should have quite similar $\delta^{13}\text{C}$ composition to that of the rocks, perhaps reflecting the same source of carbon, or low quantities of CO_2 in fluids.

The similarity of $\delta^{18}\text{O}$ values among unrecrystallized dolostone, slightly recrystallized dolostone, hydrothermal dolomite and dawsonite (Fig. 7) fits the hypothesis of derivation of oxygen involved in the formation of these two mineral phases from the same source. In agreement with these considerations, and also taking into account the order of deposition defined above, the early-deposited hydrothermal dolomite shows lower $\delta^{18}\text{O}$ values than those of late dawsonite.

The slightly higher $\delta^{13}\text{C}$ values of hydrothermal dolomite and dawsonite with respect to unrecrystallized rocks may be due to enrichment in ^{13}C of the hydrothermal fluids from which the carbonate minerals were deposited, owing to isotopic exchange during dissolution and consequently mobilization of rocks which, after re-

stage	PRIMARY			SECONDARY
	Fe-sulfide	As-Sb sulfide	carbonate-sulfate	supergene
MARCASITE	-----			
GREIGITE	-----			
QUARTZ (CHALCEDONY)		-----		
STIBNITE		-----		
REALGAR		-----		
ORPIMENT		-----		
CALCITE			-----	
DOLOMITE			-----	
DAWSONITE			-----	
ARAGONITE				---
BARITE				---
GYPSUM				---
NATIVE AS				---
GIBBSITE				---
ARSENOLITE				---
PHARMACOLITE				---
GOETHITE				---

FIG. 8. Sequence of stages of deposition and order of formation of the main mineral phases in the Koman deposit.

crystallization, had lower $\delta^{13}\text{C}$ values. Consequently, the lowering of $\delta^{13}\text{C}$ during dolostone recrystallization is consistent with the availability of isotopically heavier C upon formation of hydrothermal dolomite and dawsonite (Fig. 7).

There is little isotopic information on mineralization in Albania. Furthermore, the high $\delta^{18}\text{O}$ values of the Koman dawsonite are more akin to those of dawsonite formed at low temperatures (about 25°C) (Tanzania, Olduvai Gorge; Mauritania, Richât: Boussaroque *et al.* 1975, Baker *et al.* 1995), than those of dawsonite deposited by hydrothermal fluids (Italy, Orciatice and Piancastagnaio; Canada, McGill campus: Boussaroque *et al.* 1975) or by deep seepage circulation (Australia, Bowen–Gunnedah–Sydney: Baker *et al.* 1995) at relatively higher temperatures (60–70°C).

The oxygen isotopes of the quartz at Koman are similar to those of fluids associated with epithermal deposits formed in several continental settings. The large quantity of isotopic data reported in the literature includes deposits that occur mostly in the form of veins, disseminated in subvolcanic, volcanic and sedimentary rocks, and as replacements of limestone (O'Neil & Silberman 1974, Rye & Ohmoto 1974, Taylor 1974, Casadevall & Ohmoto 1977, Kamilli & Ohmoto 1977, Hattori & Sakai 1979, O'Neil & Bailey 1979, Sawkins *et al.* 1979, Radtke *et al.* 1980, Robinson & Christie 1980), all situations genetically similar to the case at Koman.

The $\delta^{34}\text{S}$ values of realgar and orpiment indicate that S involved in sulfide deposition may: i) have a magmatic signature ($0 \pm 2\%$; Ohmoto & Rye 1979), ii) have undergone late isotopic fractionation with enrichment of heavier S during hydrothermal processes, and iii) have undergone late involvement of S from other sources (*e.g.*, seawater 10–30‰; Schroll 1984).

The relatively high Se contents of realgar and orpiment ($\bar{x} = 0.58 \pm 0.02$ and $0.53 \pm 0.06\%$, respectively) fit the volcanic origin of the sulfur, as Se is a typical indicator of deposition in a volcanic environment (*e.g.*, Anderson 1969, Huston *et al.* 1995). Thus, according to textural relationships, the similar $\delta^{34}\text{S}$ values of realgar and orpiment support the formation of orpiment both directly from mineralizing fluids and by transformation of realgar, in any case driven by an expected increase in S_2 fugacity. The transformation of realgar (AsS) into orpiment (As_2S_3) also made As available to form the native As found in the mineralization.

The lower Se contents of early-deposited stibnite with respect to those of late-deposited sulfur-bearing arsenides are consistent with relative enrichment in Se of fluids during this late stage of the mineralizing process.

Both marcasite and greigite have low Co/Ni values, reflecting low-temperature conditions during their deposition (*e.g.*, Hawley & Nichol 1961). The relatively high As contents of marcasite, greigite and stibnite may be

due to relatively high contents of As in fluids during both Fe- and As–Sb-sulfide stages of deposition.

On the basis of the very low Mg contents of calcite, information about its temperature of deposition was obtained using the calcite–dolomite geothermometer (Bickle & Powell 1977), which gave values lower than 350°C. As regards the As–Sb-sulfide stage, the assemblage of stibnite, realgar, orpiment and native As defines temperatures of deposition of up to 75–85°C, as proposed for this association by Migdisov & Bychkov (1998). Thus, the early Fe-sulfide stage took place at temperatures above 75–85°C, and the late carbonate stage included deposition of dawsonite at temperatures probably below 75–85°C. These ranges fit those (<60°C) experimentally defined by Besson *et al.* (1973) for the formation of dawsonite. Accordingly, the paragenetic assemblage of As- and Sb-sulfides is also typical of the epithermal stage and fits an approximate temperature range of 200 to 70°C.

Origin of mineralization

The Shkodra–Pec alignment is one of the three main Albanian transversal faults (a roughly WSW–ENE trend) that played a very important role in the geological evolution and metallogenetic processes of Albania. These faults cut the Earth's crust deeply, developed as transforms (Liassic), overthrusts (Upper Jurassic-Tertiary) and normal faults (Pliocene-Quaternary) in time, and are still active today. Along and near each of these faults, epigenetic mineralization of realgar–orpiment, cinnabar, fluorite, barite, polymetallic and polysulfide, dawsonite, chrysotile and magnesite occurs. In particular, the main occurrences of dawsonite in Albania were deposited in the Koman area, along the Shkodra–Pec fault.

In the Dinarides, the combination of Tertiary magmatism (intermediate-acidic and acidic, including alkaline, rhyolitic, trachyandesitic-latic and dacitic-andesitic volcanic rocks of Oligocene to Lower Miocene age: Gjata & Kodra 1982, Grazhdani 1987) with the occurrence of high-angle faults and wallrocks receptive to mineralizing fluids seems to provide a favorable environment for the formation of many mineral deposits. Magmatic rocks of this age outcrop in Kosovo (FYRM) to the east (Grazhdani *et al.* 1989, Jankovic *et al.* 1997) along the Skodra–Pec tectonic alignment. The Alšar As–Sb–Tl–Au epithermal deposit in the Kozuf district, and the Trepča deposit, the most important polymetallic mesothermal-epithermal deposit in the Kopaonik Massif region, are both clearly linked to outcropping subvolcanic rocks of Tertiary age, whereas at Koman and the Korrab Mountains, this relationship is not evident.

These considerations, and the information collected in this study, suggest that a buried magmatic body established a hydrothermal-metasomatic system of circu-

lation of mineralizing solutions, which caused leaching of wallrocks and then deposition along pathways in tectonic contacts. The epithermal to telethermal and xenothermal features of the deposits fit the presence of a deep magmatic body. On the other hand, the Levrushku (Cretaceous? Jurassic?) and Fierza-Poravi (Middle Jurassic) intrusive rocks and the para-ophiolitic (Upper Jurassic) and mafic, trachytic-rhyolitic and andesitic-dacitic (Middle Triassic) volcanic rocks outcropping in the Koman region did not cause any hydrothermal activity in the study area, as they predate the Koman occurrences and their host rocks (Gjata & Kodra 1982).

CONCLUSIONS

The data on the Koman deposit, which oddly features dawsonite among its main minerals, suggest the following conclusions and the most probable genetic model:

1) The main paragenetic assemblages were: i) marcasite – greigite (Fe-sulfide stage); ii) quartz – stibnite – realgar – orpiment – calcite (As-Sb-sulfide stage); iii) dolomite – calcite – dawsonite – aragonite – barite – gypsum (carbonate-sulfate stage); iv) native As – gibbsite – arsenolite – pharmacolite – goethite (super-gene stage).

2) There was an important regional tectonic control during processes of deposition.

3) A local lithostratigraphic control is evident in the carbonate rocks, which show a very high reactivity with the hydrothermal fluids.

4) The $\delta^{18}\text{O}$ and $\delta^{13}\text{C}$ values of dawsonite and hydrothermal dolomite suggest a derivation by remobilization from the Koman dolostone.

5) The small amounts of circulating water, reflecting a low water:rock ratio, consequently gave rise to small-scale isotopic exchange between dolostone and hydrothermal carbonate minerals.

6) The low Co/Ni values of both marcasite and greigite reflect low-temperature conditions during their deposition.

7) The $\delta^{34}\text{S}$ values of realgar and orpiment indicate that the sulfur involved in sulfide deposition was of magmatic origin; the relatively high Se contents of these minerals are appropriate with the subvolcanic to volcanic origin of the sulfur.

8) On the basis of evidence of the magmatic origin for some of the mineralogical assemblages at Koman and of the lack of magmatic rocks (coeval to mineralization) outcropping in the area, we suggest that a buried magmatic body, probably related to the Dinaric Tertiary magmatism, activated a system of hydrothermal circulation.

9) This hydrothermal system is responsible for the formation of the Alšar, Trepča, Korrab and Koman deposits which, probably, belong to the same metallogenic

province; consequently, taking into account the mesothermal-epithermal features of the Alšar and Trepča zones of mineralization and the epithermal-telethermal features of the Koman and Korrab deposits, we also suggest that the latter two deposits occupied a distal position with respect to the magmatic source.

ACKNOWLEDGEMENTS

This work was financially supported by MURST (60%) and by the Italian Council of Research scientific projects of the “Centro di Studio per gli Equilibri Sperimentali in Minerali e Rocce” (now IGG, CNR, Rome, Italy). The authors thank referees T. Molnar and F. Punkàs, and associate editor V. Bermanec for their critical review and comments, which allowed us to improve the paper. We are grateful for the review, useful suggestions, and extensive improvement to the English by R.F. Martin. Thanks are also due to E. Bonatti for critical reading of this paper, and M. Salvati and L. Di Pietro for drawing of the sketch maps.

REFERENCES

- ANDERSON, C.A. (1969): Massive sulfide deposits and volcanism. *Econ. Geol.* **64**, 129-146.
- BAKER, J.C., BAI, G.P., HAMILTON, P.J., GOLDING, S.D. & KEENE, J.B. (1995): Continental-scale magmatic carbon dioxide seepage recorded by dawsonite in the Bowen – Gunnedah – Sydney Basin system, Eastern Australia. *J. Sedim. Res.* **A65**, 522-530.
- BESSON, H., CAILLÈRE, S., HÉNIN, S. & PROST, R. (1973): Formation expérimentale et conditions de gisement de la dawsonite. *C.R. Acad. Sci. Paris*, sér. **D**, 261-264.
- BICKLE, M.J. & POWELL, R. (1977): Calcite-dolomite geothermometry for iron-bearing carbonates: the Glockner area of the Tauern Window, Austria. *Contrib. Mineral. Petrol.* **59**, 281-292.
- BOROVA, F., PECANI, K. & STRAKOSHA, B. (1991): *Preliminary Economic Estimation Study of the Dawsonite Deposit of Koman-Puka*. Chemical Technology Institute, Ministry of Public Economy and Privatisation, Tirana, Albania, Internal Rep.
- BOUSSAROQUE, J.L., LÉTOLLE, R. & MAURY, R.A. (1975): Formation de la dawsonite des Richât (Adrar de Mauritanie): analyse isotopique ^{13}C et ^{18}O . *C.R. Acad. Sci. Paris*, **281**, sér. **D**, 1075-1078.
- CASADEVALL, T. & OHMOTO, H. (1977): Sunnyside mine, Eureka mining district, San Juan County, Colorado: geochemistry of gold and base metal ore deposition in the volcanic environment. *Econ. Geol.* **72**, 1285-1320.
- COLE, D.R. (1994): Evidence for oxygen isotope disequilibrium in selected geothermal and hydrothermal ore deposit systems. *Chem. Geol.* **111**, 283-296.

- _____ (2000): Isotopic exchange in mineral–fluid systems. IV. The crystal chemical controls on oxygen isotope exchange rates in carbonate – H₂O and layer silicate – H₂O systems. *Geochim. Cosmochim. Acta* **64**, 921-931.
- _____ & CHAKRABORTY, S. (2001): Rates and mechanism of isotopic exchange. In *Stable Isotope Geochemistry* (J.W. Valley & D. Cole, eds.). *Rev. Mineral. Geochem.* **43**, 83-190.
- DE MICHELE, V., MINUTTI, L. & SCAINI, G. (1965): Considerazioni sulla dawsonite di alcune località. *Atti Soc. Ital. Sci. Nat.* **104**, 383-391.
- FAURE, G. (1986): *Principles of Isotope Geology* (2nd ed.). John Wiley and Sons, New York, N.Y.
- FRUEH, A.J. & GOLIGHTLY, J.P. (1967): The crystal structure of dawsonite NaAl(CO₃)(OH)₂. *Can. Mineral.* **9**, 51-56.
- GJATA, K. & KODRA, A. (1982): Jurassic-Cretaceous and youngest post-ophiolitic magmatism of intermediate-acid and acid composition in Albania. *Bul. Shkenc. Gjeol.* **4**, 25-38.
- GOLDBERY, R. & LOUGHNAN, F.C. (1970): Dawsonite and nordstrandite in the Permian Berry Formation of the Sydney Basin, New South Wales. *Am. Mineral.* **55**, 477-490.
- GRAHAM, R.P.D. (1908): Dawsonite: a carbonate of soda and alumina *Trans. R. Soc. Can., Sect. IV*, **2**, 165-177.
- GRAZHDANI, A. (1987): Metallogeny of transversal faults in Albanides. *Bul. Shkenc. Gjeol.* **4**, 35-47.
- _____, ALIAJ, S.H., TUZI, H., DEDA, T. & HOXHA, V. (1989): Transversal tectonics in the Albanides and related new minerals. *Bul. Shkenc. Gjeol.* **4**, 235-247.
- _____ & BUSHATI, Z. (1983): Relationships of arsenic and dawsonite mineralizations in Koman–Bene area, North Albania. *Bul. Shkenc. Gjeol.* **2**, 103-119.
- HARRINGTON, B.J. (1874): Note on dawsonite, a new carbonate. *Can. Natural. and Quart. J. Sci.* **VII**, 305-309.
- _____ (1878): Note on the composition of dawsonite. *Can. Natural., New Ser.* **X**, 84-86.
- HATTORI, K. & SAKAI, H. (1979): D/H ratios, origins and evolution of the ore-forming fluids for the Neogene veins and Kuroko deposits of Japan. *Econ. Geol.* **74**, 535-555.
- HAWLEY, J.E. & NICHOL, I. (1961): Trace elements in pyrite, pyrrhotite and chalcocopyrite of different ores. *Econ. Geol.* **56**, 467-487.
- HAY, R.L. (1963): Zeolitic weathering in Olduvai Gorge, Tanganyika. *Geol. Soc. Am., Bull.* **74**, 1281-1286.
- _____ (1964): Phillipsite of saline lakes and soils. *Am. Mineral.* **49**, 1366-1387.
- HERITSCH, H. (1975): Dawsonit NaAl(CO₃)(OH)₂ als tiefhydrothermales Umwandlungsprodukt einer Ergußgesteinsbrekzie aus einer Tiefbohrung in der Oststeiermark (Österreich). *Neues Jahrb. Mineral., Monatsh.*, 360-368.
- HOXHA, V. (2001): *The Main Geological Features and Prospects in Kercisht–Sorocol Region (Korrab, Eastern Albania)*. Ph.D. thesis, Faculty of Geology and Mining, Univ. of Tirana, Tirana, Albania.
- HUSTON, D.L., SIE, S.H., SUTER, G.F., COOKE, D.R. & BOTH, R.A. (1995): Trace elements in sulfide minerals from Eastern Australian volcanic-hosted massive sulfide deposits. I. Proton microprobe analyses of pyrite, chalcocopyrite, and sphalerite. II. Selenium levels in pyrite: comparison with δ³⁴S values and implications for the source of sulfur in volcanogenic hydrothermal systems. *Econ. Geol.* **90**, 1167-1196.
- JANKOVIC, S., BOEV, B. & SERAFIMOVSKI, T. (1997): *Magma-tism and Tertiary Mineralization of the Kozuf Metallogenic District, the Republic of Macedonia, with Particular Reference to the Alžar Deposit*. Faculty of Mining and Geology, University of St. Kiril and Metodij (Skopje), Spec. Issue **5**.
- KAMILLI, R.J. & OHMOTO, H. (1977): Paragenesis, zoning, fluid inclusion, and isotopic studies of the Finlandia vein, Colquid district, central Peru. *Econ. Geol.* **72**, 950-982.
- LEKA, G. J., GJONI, S., DEDA, T. & LLESHI, N. (1997): Geological features, economic potentiality, perspectives and tendencies of the scientific research in the Puka region. *Albanian Geological Survey, Tirana, Albania, Internal Rep.*
- MALESANI, P. & VANNUCCI, S. (1974): Su una nuova varietà di dawsonite ritrovata nella Valle Benedetta (Livorno). *Per. Mineral.* **43**, 655-662.
- MIGDISOV, A.A. & BYCHKOV, A.Y. (1998): The behaviour of metals and sulphur during the formation of hydrothermal mercury – antimony – arsenic mineralization, Uzon caldera, Kamchatka, Russia. *J. Volc. Geotherm. Res.* **84**, 153-171.
- OHMOTO, H. & RYE, R.O. (1979): Isotopes of sulfur and carbon. In *Geochemistry of Hydrothermal Ore Deposits* (2nd edition, H.L. Barnes, ed.). John Wiley and Sons, New York, N.Y. (509-567).
- O'NEIL, J.R. & BAILEY, G.B. (1979): Stable isotope investigations of gold-bearing jasperoid in central Drum Mountain, Utah. *Econ. Geol.* **74**, 852-859.
- _____ & EPSTEIN, S. (1966): Oxygen isotope fractionation in the system dolomite – calcite – carbon dioxide. *Science* **152**, 198-201.
- _____ & SILBERMAN, M.L. (1974): Stable isotope relations in epithermal Au–Ag deposits. *Econ. Geol.* **69**, 902-909.
- PELLOUX, A. (1932): Contributo alla mineralogia Albanese. II. Minerali del giacimento a solfuri arseniacali di Komana nella Valle del Drin. *Per. Mineral.* **3**, 1-15.

- RADTKE, A.S., RYE, R.O. & DICKSON, F.W. (1980): Geology and stable isotope studies of the Carlin gold deposit, Nevada. *Econ. Geol.* **75**, 641-672.
- RIPPERDAN, R.L. (2001): Stratigraphic variation in marine carbonate carbon isotope ratios. In *Stable Isotope Geochemistry* (J.W. Valley & D. Cole, eds.). *Rev. Mineral. Geochem.* **43**, 637-662.
- ROBINSON, B.W. (1974): The origin of mineralization at the Tui mine, Te Aroha, New Zealand, in the light of stable isotope studies. *Econ. Geol.* **69**, 910-925.
- _____ & CHRISTIE, A.B. (1980): Epithermal silver–gold mineralization, Maratoto mine, New Zealand: stable isotopes and fluid inclusions. Proc. 5th Int. Assoc. on Genesis of Ore Deposits Symp., 719-730.
- RYE, R.O. & OHMOTO, H. (1974): Sulfur and carbon isotopes and ore genesis: a review. *Econ. Geol.* **69**, 826-839.
- SAWKINS, F.J., O'NEIL, J.R. & THOMPSON, J.M. (1979): Fluid inclusion and geochemical studies of vein gold deposits, Baguio District, Philippines. *Econ. Geol.* **74**, 1420-1434.
- SHALLO, M., MELO, V., XHAFI, Z., YZEIRI, D., XHOMO, A., VRANAJ, A., GJATA, T.H. & KODRA, A. (1985): Tectonic map of Albania (scale 1:200.000). Ministry of Industry and Energetics, Tirana, Albania.
- SCHROLL, E. (1984): Geochemical indicator parameters of lead–zinc ore deposits in carbonate rocks. In *Syngeneses and Epigenesis in the Formation of Mineral Deposits* (A. Wauschkuhn *et al.*, eds.). Springer-Verlag, Berlin, Germany (294-305).
- SHEPPARD, S.M.F. & SCHWARCZ, H.P. (1970): Fractionation of carbon and oxygen isotopes and magnesium between co-existing metamorphic calcite and dolomite. *Contrib. Mineral. Petrol.* **26**, 161-198.
- SMITH, J.W. & MILTON, C. (1966): Dawsonite in the Green River Formation of Colorado. *Econ. Geol.* **61**, 1029-1042.
- SVERJENSKY, D.A. (1981): Isotopic alteration of carbonate host rocks as a function of water to rock ratio – an example from the Upper Mississippi Valley zinc–lead district. *Econ. Geol.* **76**, 154-157.
- TAN, F.C. & HUDSON, J.D. (1971): Carbon and oxygen isotopic relationships of dolomites and coexisting calcites, Great Estuarine Series (Jurassic), Scotland. *Geochim. Cosmochim. Acta* **35**, 755-767.
- TAYLOR, H.P., JR. (1974): The application of oxygen and hydrogen isotope studies to problems of hydrothermal alteration and ore deposition. *Econ. Geol.* **69**, 843-883.
- VEIZER, J. & HOEFS, J. (1976): The nature of O¹⁸/O¹⁶ and ¹³C/¹²C secular trends in carbonate rocks. *Geochim. Cosmochim. Acta* **40**, 1387-1395.
- WOPFER, H. & HOCKER, C.F.W. (1987): The Permian Groeden Sandstone between Bozen and Meran (northern Italy), a habitat of dawsonite and nordstrandite. *Neues Jahrb. Geol. Paläont., Monatsh.*, 161-176.
- XHOMO, A., KODRA, A., DIMO, L. L., SHALLO, M., VRANAJ, A., XHAFI, Z., NAKUÇI, V., YZEIRI, D., NAZAJ, S.H. & SADUSHI, P. (2002): Geological Map of Albania (scale 1:200.000), Ministry of Industry and Energetics, Tirana, Albania.

Received April 7, 2002, revised manuscript accepted March 17, 2003.